

CASTABILITY OF 718PLUS® ALLOY FOR STRUCTURAL GAS TURBINE ENGINE COMPONENTS

Benjamin Peterson¹, Venkatesh Krishnan¹, Dave Brayshaw², Randy Helmink³, Scott Oppenheimer⁴, Eric Ott⁵, Ray Benn⁶, Michael Uchic⁷

¹Honeywell Aerospace; 111 S. 34th Street; Phoenix, AZ 85034, USA

²PCC Structural; 4600 SE Harney Dr, Portland, OR 97206, USA

³Rolls-Royce; 2001 South Tibbs Ave, Indianapolis, IN 46241, USA

⁴ATI-Allvac; 2020 Ashcraft Ave, Monroe, NC 28111, USA

⁵GE Aviation; 1 Neumann Way, Cincinnati, OH 45215, USA

⁶Pratt & Whitney; 400 Main Street, E. Hartford, CT 06108, USA

⁷AFRL/RXLM, 2230 10th Street, Wright-Patterson AFB, OH 45433, USA

Keywords: 718Plus® Alloy, Castability, Weldability

Abstract

Recent developments from the cast 718Plus® Metals Affordability Initiative (MAI) program will be presented and discussed. The objective of the program is to investigate and enable the use of 718Plus® alloy in the form of investment castings by (1) increasing the allowable operating temperature by about 75°F as compared with conventional cast Alloy 718 and (2) achieve approximately 25 percent cost savings as compared with cast Waspaloy. This program builds on the successful MAI program for wrought 718Plus alloy. This technology will be implemented for the manufacture of gas turbine structural components including: combustor plenums, stator cases, diffuser cases, turbine cases, turbine frames, and other various high-strength/high-temperature structural castings. An overview of the results from the castability, weldability, and initial mechanical property investigations will be discussed. A preliminary cost benefit to aerospace components after implementation is predicted to be substantial. This recent work has warranted further investigation through the MAI program.

718Plus® is a registered trademark of ATI Properties, Inc.

Introduction

As modern gas turbine engine component temperatures continue to increase, the utility of conventional Alloy 718 is being exhausted. Conventional Alloy 718 is limited in temperature capability to 1200°F due to its principal strengthening precipitate, γ' . Above 1200°F, Alloy 718 overages, transforming the γ' (Ni₃+Nb-Al-Ti) to the equilibrium δ (Ni₃Nb) phase with an associated debit in mechanical properties and performance [1]. Current alternatives to Alloy 718 for low cost, high-temperature investment-cast structural components are limited and will challenge future cost targets for the industry. As the temperature requirements for higher-performance gas turbine engines continue to increase, the role of Alloy 718 in future engine designs will be restricted to lower temperature components, causing increased usage of more expensive alternatives such as Waspaloy. Waspaloy is significantly more expensive than conventional Alloy 718, not only because of its more expensive elemental chemistry, but also because of the relative difficulty in processing. A comparison of the chemistry of Alloy 718, 718Plus alloy, and Waspaloy is provided in Table I. In the investment cast form, Waspaloy

presents several challenges resulting in casting defects. Waspaloy is also difficult to weld and must be solution heat treated subsequent to repair, causing dimensional distortion upon cooling to room temperature. Alloy 718Plus has been developed as a cast/wrought alloy offering the cost structure of conventional Alloy 718 and the temperature capability of Waspaloy.

Table I. Chemistry of Alloy 718, 718Plus alloy, and Waspaloy.

Alloy	Ni	Cr	Co	Mo	W	Nb	Al	Ti	Fe	C	P	B
IN718	52.50	19.00	--	3.00	--	5.15	0.60	0.90	18.50	0.040	0.007	0.003
718Plus	52.00	18.00	9.10	2.70	1.00	5.40	1.45	0.75	9.50	0.020	0.006	0.005
Waspaloy	58.70	19.40	13.30	4.30	--	--	1.30	3.00	--	0.035	0.006	0.006

Alloy 718Plus is a γ' -strengthened alloy, and like other γ' -strengthened alloys, such as Waspaloy, exhibits greater thermal stability [1, 2]. The excellent relative fabricability, including weldability, of conventional Alloy 718 is owed much in part to the slow precipitation of the γ' phase [3]. Alloy 718Plus is expected to have faster precipitation kinetics than conventional Alloy 718, which may complicate casting, welding, and thermal mechanical processing. However, the γ' precipitation in 718Plus alloy is much slower than Waspaloy, most likely due to its high Nb content, which has a much slower diffusion rate [2]. Consequently, as a result of its precipitation kinetics, 718Plus alloy is an attractive potential investment-cast alloy offering increased temperature capability relative to conventional Alloy 718.

Recent work within the Metals Affordability Initiative (MAI) program has evaluated the castability and weldability of 718Plus alloy and optimized the composition for mechanical properties to determine commercial feasibility. The goals for the program were to investigate and enable the use of 718Plus alloy in the form of investment castings by (1) increasing the allowable operating temperature by about 75°F as compared with conventional cast Alloy 718 and (2) achieve approximately 25 percent cost savings as compared with Waspaloy. This program builds on the successful MAI program for wrought 718Plus alloy [4].

An investment castable 718Plus alloy represents a pervasive improvement for the gas turbine industry. The 718Plus investment casting technology will be implemented for the manufacture of gas turbine structural components such as: combustor plenums, stator cases, diffuser cases, turbine cases, turbine rear frames, and other various high-strength/high-temperature structural castings currently manufactured from Waspaloy, conventional Alloy 718, or other similar proprietary alloys, such as René 220 or RS5 [3, 5]. A typical gas turbine component application is illustrated in Figure 1. Alloy 718Plus should enable Alloy 718 components to operate at higher temperatures at a lower cost, providing a means for the gas turbine industry to continue to meet on-going cost and performance improvement goals.



Figure 1. Honeywell GTCP36-150[BH] APU combustor plenum fabricated from Alloy 718 for U.S. Army, USAF, U.S. Navy and Coast Guard variants of the Sikorsky Blackhawk helicopter.

Experimental

Thermodynamic Simulations

Thermodynamic simulations were run with the commercial JMatPro (Sente Software) software to virtually test elemental composition effects on key casting parameters such as the liquidus, the solidus, the derived freezing zone (liquidus – solidus), the gamma prime solvus, and the delta solvus temperatures. This was done to target specific elements that may have significant impact on the castability of 718Plus alloy. Of the significant elements, C, W, Co, Fe, Nb, Ti, and Al were each examined at three levels for a total of 2187 different chemistries. Ni was used as the balance element. B and P were not examined due to limitations of the simulation software. From previous work, Cr tends to influence melt phenomena in the same way as Fe, hence, the less expensive Fe was chosen to model. Mo was not examined since it should have limited influence on the secondary phases or melt characteristics as a solid solution strengthener. Table II lists the examined elements and the three compositional levels.

Table II. List of Elements and Levels Chosen for Thermodynamic Evaluation (Shaded).

718+	Nominal (Wt%)	Min.	Middle	Max.
C	0.02	0.02	0.06	0.1
Mo	2.70			
W	1.0	1	1.5	2
Cr	18.0			
Ni	Bal			
Co	9.10	8	9	10
Fe	9.50	9	10	11
Nb	5.45	5.0	5.75	6.5
Ti	0.75	0.75	0.85	0.95
B	0.0050			
P	0.008			
Al	1.49	1.45	1.65	1.95

Hot Tear and No-Fill DOE

Based on the results from the thermodynamic simulations, multiple numerical evaluations were employed to study the castability of chemistry variants of 718Plus alloy. A 10,000 pound master heat ingot was produced with a nominal chemistry. Elemental additions were made to subsequent castings from the master heat ingot via the lost wax method to achieve target chemistry variations. Pour and mold temperatures were held constant during the trials for all alloys and were not optimized for the various alloy compositions during this feasibility effort. A hot tear mold (Figure 2a) was used to characterize the hot tear susceptibility, where the total hot tear length was reported. Total hot tear length is a sum of all the crack lengths, found by Fluorescent Penetrant Inspection (FPI), on all arms from each hot tear casting. A non-concentric ring mold (Figure 2b) was used to characterize filling capabilities, where the percent of no-fill area is reported. Alloys considered castable show less susceptibility to hot tear formation and have less no-fill area.

Table III lists the mechanical property test conditions for each of the five down-selected alloys. The 1300°F test temperature represents a target application temperature for the developed alloy. Plates 10x4x5/8 inch plates of each composition were cast for mechanical test specimens.

Table III. Mechanical Property Assessment Test Conditions.

Test Type	Test Temp. (°F)	Test Conditions	Repeats per Condition	Test Standard
Tensile Testing	800, 1200, 1300	N/A	3	E-21
Stress Rupture (combo bar)	1300	85 ksi	3	E-292
Creep Rupture	1300	85 ksi	3	E-139
Low-cycle fatigue (LCF)	1300	0.45 % strain; R-ratio=0; 20cpm	5	EIS 1888/E-606

Creep rupture coupons were traditional dog-bone samples. Stress rupture coupons were combo bar samples with a straight-sided, dog-bone gage combined with a notch, to differentiate the notch sensitivity between the alloys. Tests that fail at the notch, instead of the gage, may have increased notch sensitivity. It is important to note that stress rupture samples are sensitive to machining which may be a source of error in distinguishing notch sensitivity properties. Low cycle fatigue (LCF) tests were conducted in air with strain control using closed loop servo-controlled hydraulically actuated test machines. The specimens were heated by high frequency induction. Temperature was held constant for each test to the final failure or removal of the test specimen. Frequency, R-Ratio, total strain range (strain controlled mode), and/or peak stress (load controlled mode) were controlling parameters. If a specimen reached 120,000 cycles without crack initiation, the test was suspended and switched to load control at 10 Hz using the measured maximum and minimum stress range from the last strain-controlled cycle as the applied load, and run to failure or 1,000,000 cycles, whichever occurred first.

Results and Discussion

Thermodynamic Simulations

Thermodynamic properties of the liquidus, solidus, gamma prime solvus, and delta solvus were analyzed with Minitab and appeared to be primarily first order effects. Main effects plots were used to examine the elemental relationships independently of each other in Figures 4-6. The freezing zone (liquidus minus solidus) results show that Nb, C, and Fe have the largest effect, which is indicative of how much time the solidification process may take, how much elemental segregation may be expected, propensity for cavity formation, and hot tear propensity. Al, Ti and Nb affect the gamma prime solvus, with limited interaction effects. Al, C, and Nb affect the delta solvus. Co and W do not have significant effects on casting performance, hence, were not varied during subsequent experimental investigations.

In all of the thermodynamic work it is important to note that the results were first order (single element), and linear over the examined compositional range. These simulation results warranted a two-level DOE of the significant elements during the castability assessment to further investigate elemental effects on casting performance.

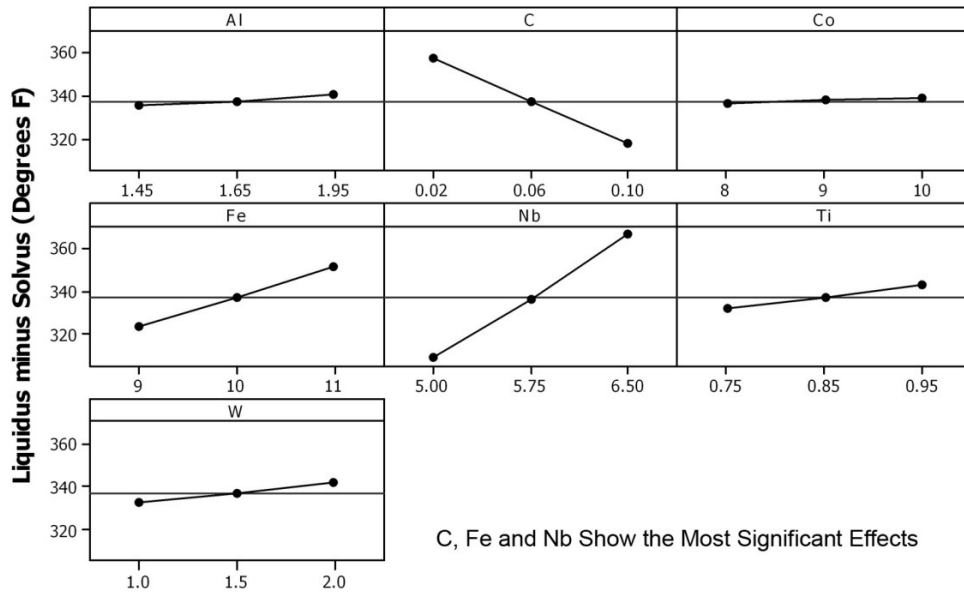


Figure 4. Main effects plot for Freezing Range vs. Elemental (wt%).

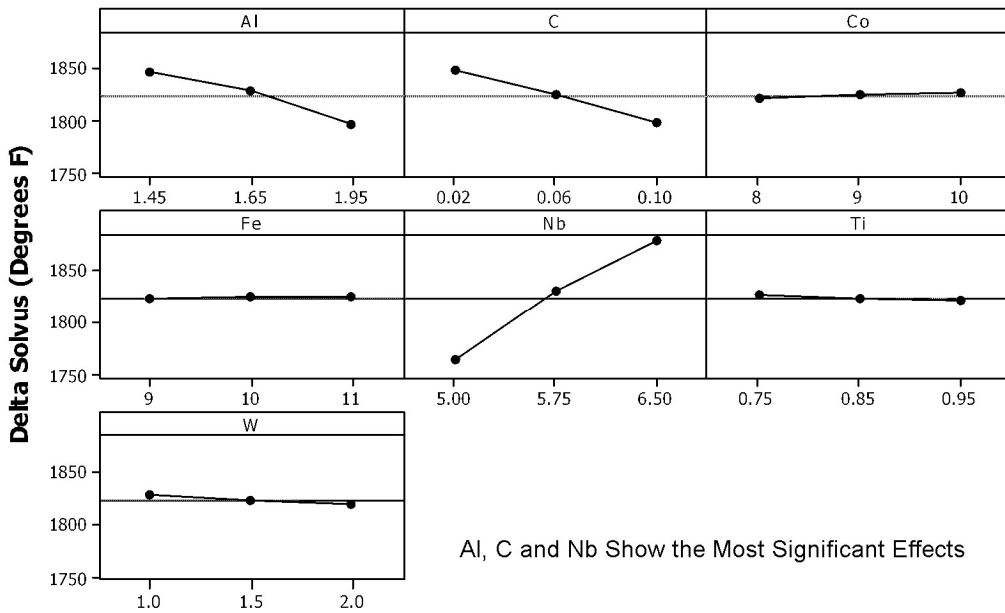


Figure 5. Main effects plot for Delta Solvus vs. Elemental (wt%).

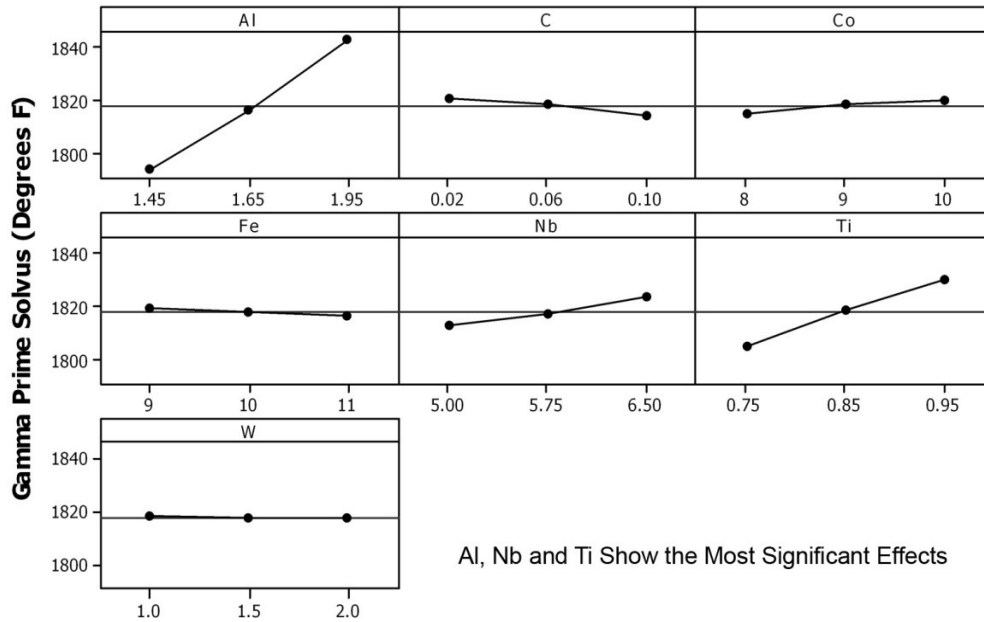


Figure 6. Main effects plot for Gamma Prime Solvus vs. Elemental (wt%).

Hot Tear and No-Fill DOE

Several castings (32), based on the JMatPro simulations, were poured into the hot-tear and no-fill molds via two separate Designs of Experiment (DOE) that examine compositional effects on castability. The first DOE (2-level) varied C, Nb, Ti, Al, Fe, and B per the compositions in Table IV. Per the Pareto charts in Figure 7, Carbon was the only element showing a statistically significant effect on hot tear length. No elements showed statistically significant effects on mold filling capabilities. Subsequently, a second DOE only varied C, Nb, Ti, and Al (3-level) (see Table IV). Nb, Ti, and Al remained in the DOE due to their effect on mechanical properties. Fe and B were held at constant levels produced in the master heat because of their lack of statistical significance in the first DOE.

The hot tear and no-fill results from the second DOE were added to the results from the first DOE and the same statistical analysis was performed to identify significant casting elements. Figure 8 shows that the carbon, carbon-niobium, and titanium-niobium interactions, in addition to carbon, affect hot tear propensity. Aluminum is the only element showing a statistically significant role in the filling capabilities of the alloy.

The two sets of DOEs performed represent a substantial amount of work to understand the key compositional parameters for 718Plus castability. From the casting of the hot tear and percent no-fill molds, it was concluded that all investigated alloys are castable. The results were comparable to other alloys currently used in production of parts at PCC Structurals. It was also found that increasing carbon levels reduces hot tear formation and increasing aluminum levels decreases the filling capability of the alloy. In addition to understanding the general castability aspects of 718Plus alloy, compositions optimized for castability were chosen for subsequent weldability and mechanical property assessments.

Table IV. Chemistry Target Variations of both DOEs (Molds 1-16 correspond to the first DOE, and 17-32 correspond to the second DOE).

Mold	Carbon	Niobium	Titanium	Aluminum	Iron	Boron
1	0.02	5	0.75	1.85	11	0.01
2	0.1	6.5	0.95	1.45	9	0.005
3	0.1	5	0.75	1.85	9	0.01
4	0.02	6.5	0.95	1.45	11	0.005
5	0.1	6.5	0.75	1.85	9	0.005
6	0.02	5	0.75	1.45	9	0.005
7	0.1	5	0.95	1.45	9	0.01
8	0.02	5	0.95	1.45	11	0.01
9	0.02	5	0.95	1.85	9	0.005
10	0.02	6.5	0.95	1.85	9	0.01
11	0.1	6.5	0.75	1.45	11	0.01
12	0.02	6.5	0.75	1.85	11	0.005
13	0.1	6.5	0.95	1.85	11	0.01
14	0.1	5	0.75	1.45	11	0.005
15	0.1	5	0.95	1.85	11	0.005
16	0.02	6.5	0.75	1.45	9	.01
17	0.02	5	0.75	1.45	9	0.005
18	0.02	5.75	0.75	1.65	9	0.005
19	0.06	5	0.85	1.45	9	0.005
20	0.02	5	0.85	1.65	9	0.005
21	0.06	5.75	0.75	1.45	9	0.005
22	0.06	5	0.75	1.65	9	0.005
23	0.06	5.75	0.85	1.65	9	0.005
24	0.02	5.75	0.85	1.45	9	0.005
25	0.1	6.5	0.85	1.65	9	0.005
26	0.06	5.75	0.85	1.65	9	0.005
27	0.1	5.75	0.95	1.65	9	0.005
28	0.1	5.75	0.85	1.85	9	0.005
29	0.06	6.5	0.85	1.85	9	0.005
30	0.06	5.75	0.95	1.85	9	0.005
31	0.06	6.5	0.95	1.65	9	0.005
32	0.1	6.5	0.95	1.85	9	0.005

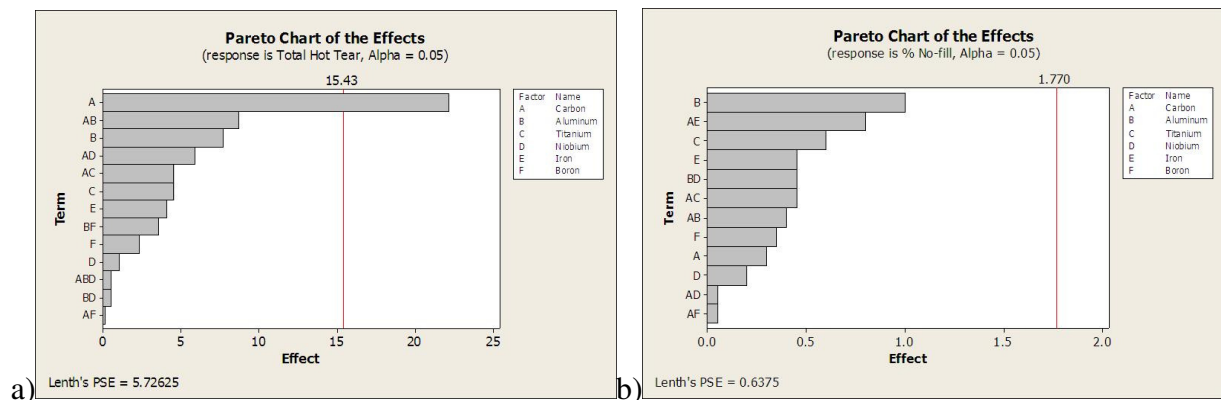


Figure 7. Pareto charts from the first castability DOE showing (a) C as the only major element playing a statistically significant role in hot tear formation and (b) no elements with statistically significant roles in filling capabilities.

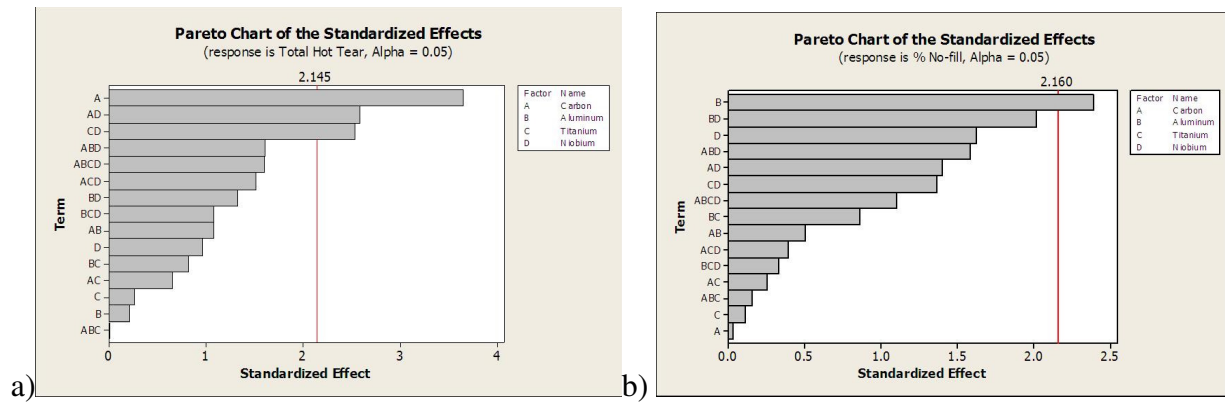


Figure 8. Pareto charts showing (a) carbon, carbon-niobium, and titanium-niobium having a statistically significant role in the formation of hot tears and (b) aluminum as the only element playing a statistically significant role in filling capabilities.

Weldability and Mechanical Property Assessment

Table V lists the measured compositions of the five down-selected compositional variants chosen for the mechanical property assessment. Figure 9 represents the solution space chosen to examine a range of hardener content. For example, alloy C has increased hardener content (Al, Nb, and Ti), targeting increased strength. Alloy E has reduced hardener content, targeting improved weldability. Alloys A, B, and D examine the solution space between alloys C and E.

Table V. Actual Cast 718Plus Chemistries for Weldability and Mechanical Test Trials (wt %).

Target	Alloy	C	Al	Ti	Nb
	A	0.05	1.58	0.75	6.67
	B	0.05	1.57	0.86	5.94
Strength	C	0.05	1.78	0.84	6.65
	D	0.05	1.36	0.76	6.65
Weldability	E	0.03	1.37	0.77	5.98

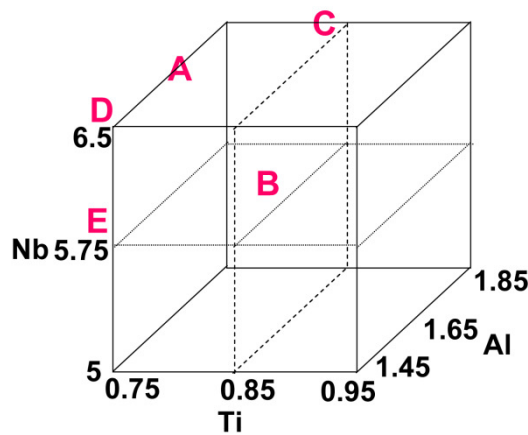


Figure 9. Representation of the five down-selected chemistries in 3-D solution space (measured compositions, wt %), depicting the range of hardener content (Al, Nb, and Ti).

Thermodynamic modeling of each composition was performed to select the heat treat solution temperature for each of the five down-selected compositions. The solution temperature was set 100 to 130°F below the calculated delta solvus for each composition. Table VI describes the heat treatment performed for each alloy in a vacuum furnace prior to sample machining.

Table VI. Heat treat parameters for the five down-selected compositions.

Alloy	Heat Treatment	
	Solution Temp (°F)	Age (°F)
A	1800, 1 Hour	1450, 8 Hrs/1300, 8 Hrs
B	1760, 1 Hour	1450, 8 Hrs/1300, 8 Hrs
C	1780, 1 Hour	1450, 8 Hrs/1300, 8 Hrs
D	1800, 1 Hour	1450, 8 Hrs/1300, 8 Hrs
E	1760, 1 Hour	1450, 8 Hrs/1300, 8 Hrs

Weldability Assessment

Based on the heat treat schedules in Table VI, samples from the 5 down-selected alloys were heat treated and evaluated in each of the (1) solution and (2) solution-plus-aged conditions. No homogenization was performed on the samples for weld testing, which may accentuate segregation-related weld effects in these screening tests. After EB welding of the picture frame coupons, samples were cut in half and one-half was aged, in order to assess both the as-welded and as-welded-plus-aged conditions.

Figure 10a shows a cross-section view of a typical weld, where the plane of polish used to assess for weld defects (by polishing down into the weld from the sample surface) is shown in this figure. This location represents the region of the weld with the highest likelihood of weld-related cracks. The total crack length per unit weld length was determined and is shown in Figure 10b. As with many weldability type test methodologies, the potential for test result variability due to local microstructure (grain size, etc.) must be considered in drawing conclusions on the overall weldability. Since the amount of weld material evaluated was small and some variation in local microstructure could be present, the assessment performed in this set of tests was approximate and makes the assumption that these microstructure variability effects are not significant enough to affect the overall rank ordering of the alloys.

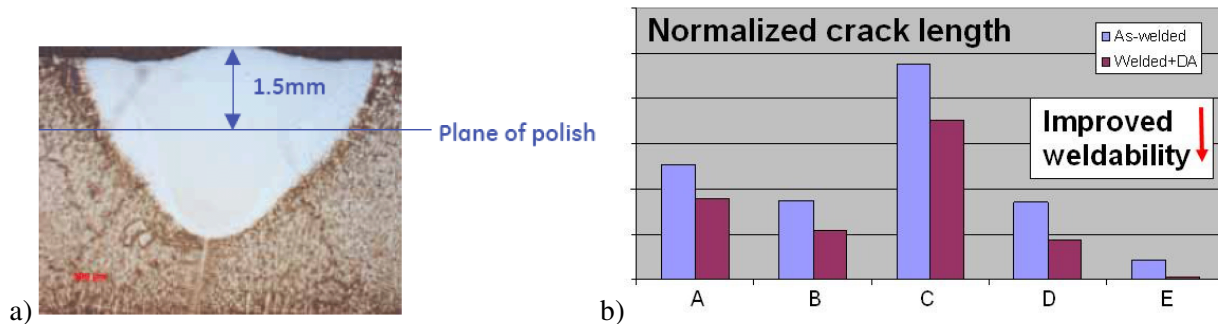


Figure 10. (a) Location of EB weld section used for assessment of crack length per unit weld length (b) relative weldability of alloys based on EB weld coupon testing assessment of crack length per unit weld length.

In summary, all 5 alloys in 2 initial heat treatment conditions welded without visual or macroscopic defects. No significant evolution of volatiles or defects was apparent during welding, suggesting that the material was relatively clean. Samples evaluated in the as-welded condition were noted to have varying degrees of grain boundary liquation in the heat affected zone and resulting liquation cracking. A ranking (below) of the relative severity of cracking by this mechanism resulted in alloy E having the best weldability, as expected due to the lower hardener content. This ranking was used to discriminate between the weldability of the alloys.

E < D & B < A < C in total crack length.

Mechanical Property Assessment

Tensile Results: Figure 11 contains a summary of the average tensile values. In general, alloys A, C and D had the highest strength (yield stress and UTS). Alloys B, D and E exhibit the highest elongation values at 800 and 1200°F. Alloys A, D and E exhibit the highest elongation values at 1300°F.

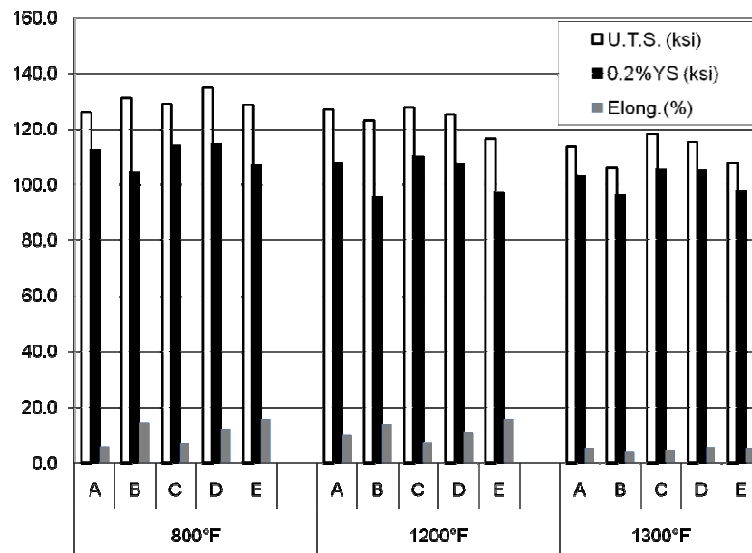
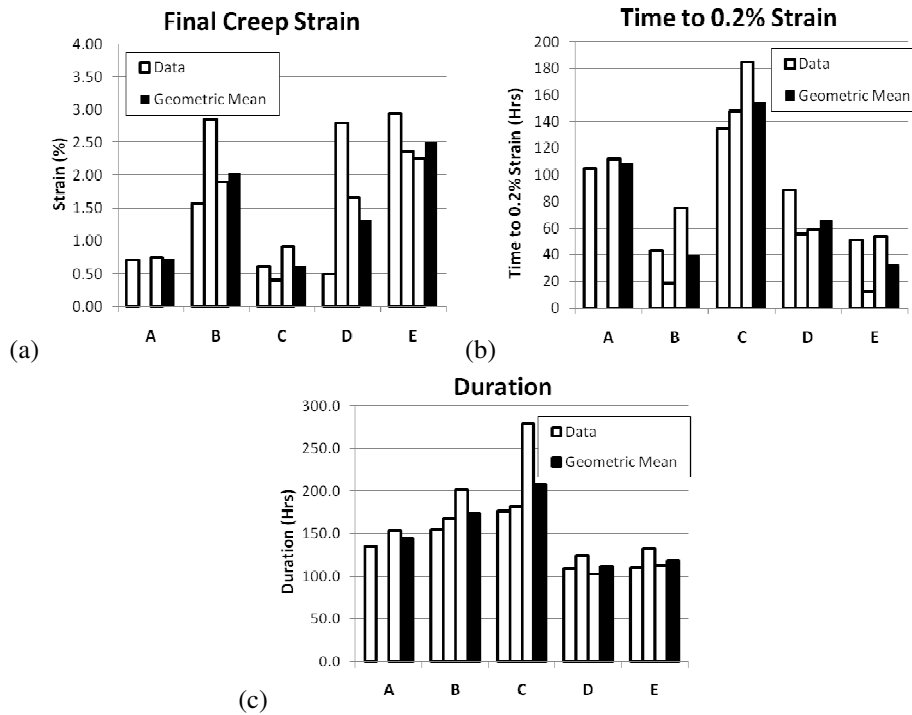


Figure 11. Summary of the average tensile results for Alloys A-E.

Creep Results: Figure 12 contains graphical representations of the creep rupture data, including time to 0.2% strain, final creep strain, and test duration. The geometric mean ($=\sqrt[n]{y_1 y_2 \dots y_n}$) is also plotted with the data for reference. Alloys A and C have the longest times to 0.2% strain and lowest final creep strains. Figure 13 is the stress rupture data plotted to distinguish between samples that failed in the gage versus the notch. All samples from alloys A and B failed in the notch. Alloy D has the least notch sensitivity, with only one of three tests failing in the notch.



Figures 12. Creep rupture results (a) final creep strain (b) time to 0.2% creep strain (c) hours of test duration. Tests performed at 1300°F and 85 ksi.

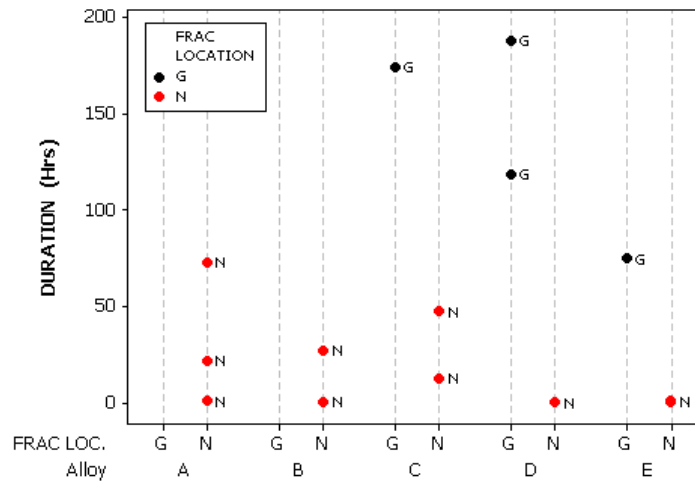


Figure 13. Combo bar stress rupture test duration (hours), distinguishing fracture location. Tests performed at 1300°F and 85 ksi.

Low Cycle Fatigue (LCF) Testing: Results were converted to a Walker Strain (Equation 1), with an assumed m value of 0.5 because of a difference in strain range.

$$\epsilon_w = (\sigma_{\max.}/E) * (\Delta\epsilon_T * E / \sigma_{\max.})^m \quad (1)$$

precipitated to mitigate notch failures. Lowering the solution temperature is predicted to precipitate more grain boundary delta which may reduce notch failures in the combo stress rupture coupons.

The solution temperature of Alloy D was lowered from 1775 and 1750°F for one hour and aged (1450°F/8 hour + 1300°F/8 hour). Additional creep and stress ruptures tests were performed. All stress rupture samples failed in the gage, which indicates that the reduced solution treat temperature, as expected, correspondingly reduces notch sensitivity. In addition, the creep rupture results show that the lower solution treat temperatures did not significantly affect the time to 0.2% strain (Figure 16).

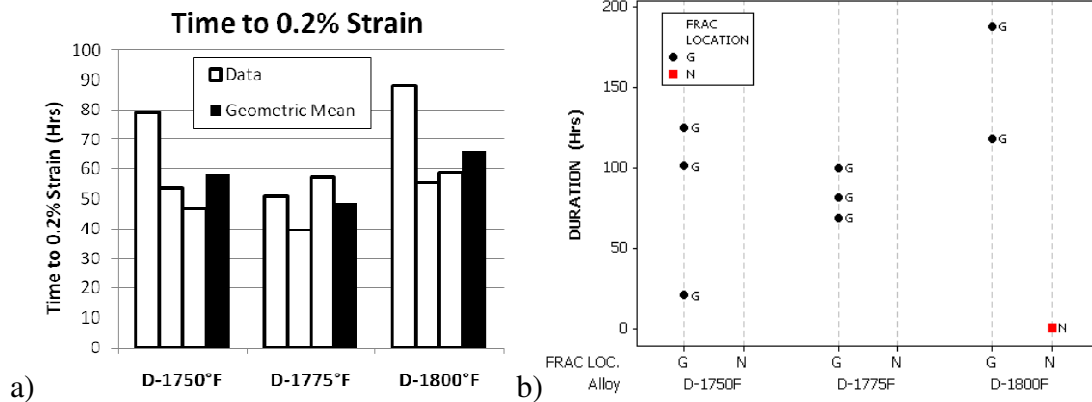


Figure 16. (a) Creep data for the additional δ precipitation tests and (b) results of the additional stress rupture tests of Alloy D.

This data confirms that optimizing the heat treat parameters can improve the mechanical properties. In this case, lowering the solution treat temperature reduced the notch sensitivity. Figure 17 is the relationship between the predicted amount of delta (JMatPro software) and the average stress rupture ductility, which shows that the amount of delta affects the notch sensitivity.

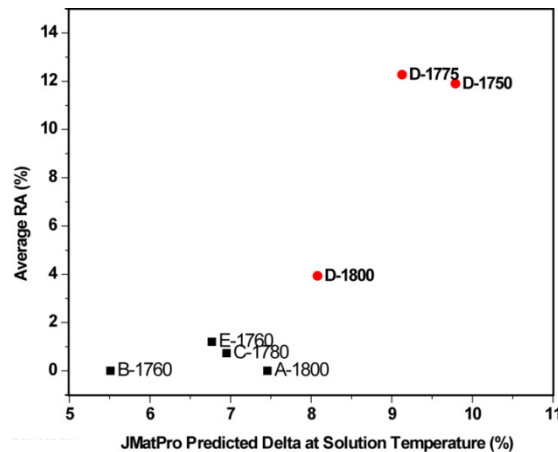


Figure 17. Plot of average ductility as a function of the predicted delta phase composition.

Chemistry Down-Select: A single target chemistry was chosen for further development during subsequent tasks of the MAI project based on the current castability, weldability, and initial mechanical property assessments. The castability and weldability assessments concluded that, in general, all of the five down-selected compositions are castable and weldable. The mechanical property data was used as the key discriminator for the final compositional down-select. An assigned ranking system was employed to protect OEM proprietary information such as design database and engine applications. Each OEM ranked the mechanical property results (ETT, Creep, LCF) of each alloy as low risk (green), medium risk (yellow) or high risk (red), with high risk (red) equating to unacceptable. Alloy D was selected for further development because it did not receive any high risk votes and ranked higher than the other alloys.

A preliminary business case for 718Plus cast parts by the MAI team has shown potential raw material, processing, and rework cost savings as compared with Waspaloy as the baseline.

Conclusion

Hot Tear and No-Fill DOEs have shown that down-selected alloy compositions are castable. These alloys weld better than Waspaloy, but worse than Alloy 718. A down-selected composition for further development has been selected, primarily based on a mechanical property assessment.

Future work is to include a heat treat optimization, further characterization of the alloy by understanding the microstructural stability and mechanical properties, and refinement of the business case.

Acknowledgments

The authors would like to acknowledge partial funding support for this effort under the U.S. Air Force Metals Affordability Initiative program, agreement no. FA8650-06-2-5211, as well as collaborative efforts under this MAI project between ATI Allvac, GE, Honeywell Aerospace, PCC Structurals, Pratt & Whitney, and Rolls-Royce.

References

1. R. L. Kennedy, "Allvac® 718Plus™, Superalloy for the Next Forty Years." *Superalloys 718, 625, 706 and Derivates 2005*, p.1. E. A. Loria, ed. TMS 2005.
2. Wei-Di Cao, "Solidification and Solid State Phase Transformations of Allvac® 718Plus™ Alloy." *Superalloys 718, 625, 706 and Derivatives 2005*. p. 165. E. A. Loria, ed. TMS 2005.
3. R. E. Schafrik, D. D. Ward, and J. R. Groh, "Application of Alloy 718 in GE Aircraft Engines: Past, Present and Next Five Years." *Superalloys 718, 625, 706 and Various Derivatives 2001*, p. 1. E. A. Loria, ed. TMS (The Minerals, Metals & Materials Society), Warrendale, PA 15086-7528, 2001.
4. E.A. Ott, J. Groh, and H. Sizek."Metal Affordability Initiative: Application of Allvac Alloy 718Plus® for Aircraft Engine Static Structural Components." *Superalloys 718, 625, 706 and Derivatives 2005*, E.A. Loria, ed. The Mineral Metals and Materails Society, 2005.

5. D. F. Paulonis and J. J. Schirra, "Alloy 718 at Pratt and Whitney – Historical Perspective and Future Challenges." Superalloys 718, 625, 706 and Various Derivatives 2001, p. 13. E. A. Loria, ed. TMS 2001.
6. W. D. Cao, "Nickel-Base Alloy", U.S. Patent 6,730,264 B2, 04 May 2004.